Focusing X-rays using Micro-Pore Optics

J. L. Catenza [*] *and C. Solans Sánchez* [†]

Abstract
This paper investigates the focusing capabilities of Micro-Pore Optics (MPOs) on X-rays by using MALTA as a detector. In this research, a Photonis micro-Xray source operated at 12 kV was used. Experiments were carried out to determine the effects of source-detector distance and MPO-source distance on the X-ray beam. The MPOs affected the hits detected by MALTA and also the divergence of the photons. A single MPO can decrease the number of hits by a factor 10^1. The divergence angle is calculated from the standard deviation of the photon detection image on MALTA. Furthermore, three set-ups were evaluated to determine which is the most effective in focusing X-rays.

Keywords
Micro-Pore Optics; MALTA; X-rays

1 Introduction

There are a lot of applications for X-rays. The use of X-ray ranges from medicine to industry. One notable application of micro-focused X-ray is imaging [1]. However, just like a conventional computed tomography scan, the sample is exposed to a greater amount of radiation. In case the sample only needs to be viewed in 2D, micro X-rays are used. This ensures that the sample is exposed to a small amount of radiation. Aside from this, micro X-rays are used in detecting small cracks in materials, gauging the accurate thickness of objects, and analyzing small sample areas with the process called Micro X-ray Fluorescence.

1.1 Focused X-rays

In any diagnostic or imaging procedure, it is important to make sure that the image that was produced due to the exposure of radiation is of high quality. By high quality means that there is a high image resolution. The spatial resolution of an X-ray film is affected by the focal spot [1]. Figure 1 shows the image formation process of two X-ray sources– (A) point source and (B) distributed source. The geometry terms are as follows:

1. SOD— Source-object distance
2. SDD— Source-detector distance
3. ODD— Object-detector distance
4. F— Focal spot distribution of the source

Looking at similar triangles, it can be shown that magnification (M) is

$$M = \frac{SDD}{SOD} \,. \tag{1}$$

In B, blurring of object is caused by focal spot distribution incident on the detector. The amount of blur can be qualified in this diagram by the size of the penumbra. The bigger the penumbra, the more blurring

[*] University of Santo Tomas, Manila, Philippines
[†] CERN, EP Department

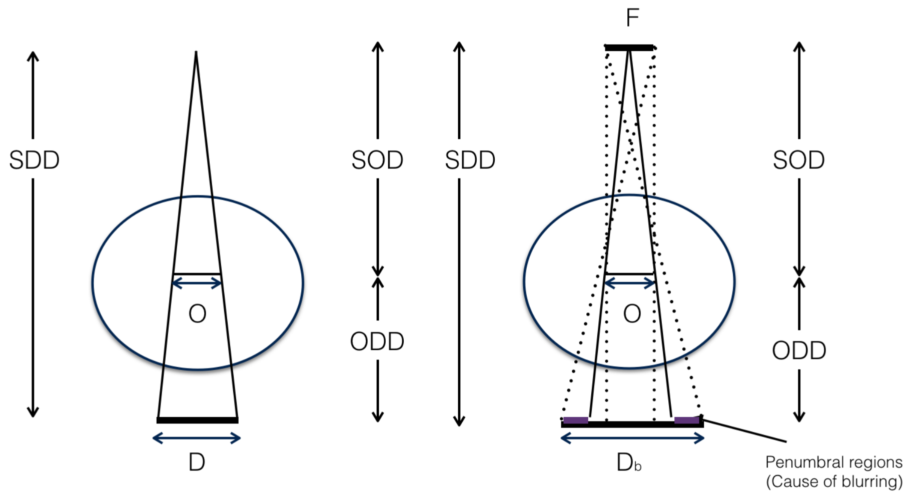

Figure 1: Visualization of Relationship Between Focal Spot Size and Penumbral Area

will occur. The size of the penumbral region increases with magnification for given focal spot size. The magnification of the object also increases with F. Thus, the bigger the focal spot, the more apparent the penumbral region is. Same as milli-focus X-ray sources, X-ray sources with a focus size in units of microns are called micro-focus X-ray sources. They are used for fluoroscopy where high resolution is required. When trying to make judgments based on visual information, there is a clear difference between systems that use high resolution and those that do not. High-resolution micro-focus X-rays produce clear images, which make it easier to find small defects and abnormalities in parts, materials, and food. Because of this, the X-ray that should bombard a sample should be as focused as possible to keep the image sharp.

1.2 MALTA

The detector used in this experiment is MALTA. This is a Monolithic Active Pixel Sensor (MAPS) [2] manufactured in Tower 180 nm technology. The characterization of this pixel detector is a very important for the development of Monolithic Pixel detectors for HL-LHC and beyond.

1.3 Micropore Optics

The MPOs used in this research are made to be used in X-Ray imaging applications. These MPOs are fabricated to have a perfect square channels to allow photons to be either focused or collimated using the concept of total external reflection at a grazing angle of less incidence. The development of these MPOs is a groundbreaking achievement especially for high energy astrophysics [3].The primary use of these MPOs is for X-ray spectroscopy for outer space application. Using these MPOs for micro X-ray focusing is what was tested in this paper.

1.4 Micro X-ray Production

X-rays are produced using a 16 mm long tube with a photo-cathode and anode made up of Chromium and Copper on top of a Beryllium window. Electrons are emitted from the photo-cathode by means of the photo-electric effect induced by a laser beam. These electrons are accelerated using 12 kV electric field applied on the tube. X-rays (bremstrahlung and fluorescence) are produced as these electrons approach the target. Figure 2 summarizes the X-ray production. The X-rays that are emitted are randomly travelling in space.

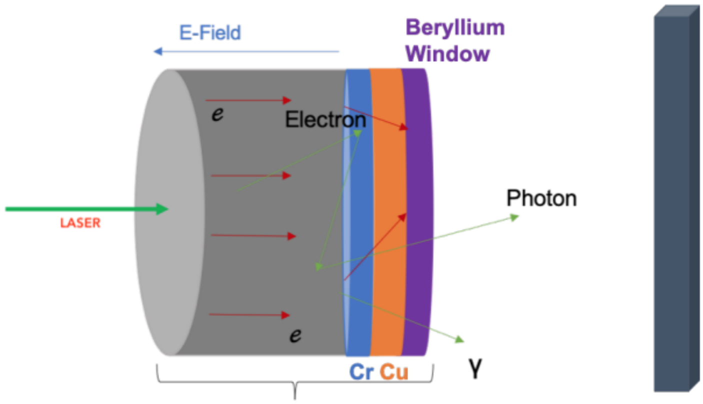

Figure 2: Visualization of Micro X-ray Production

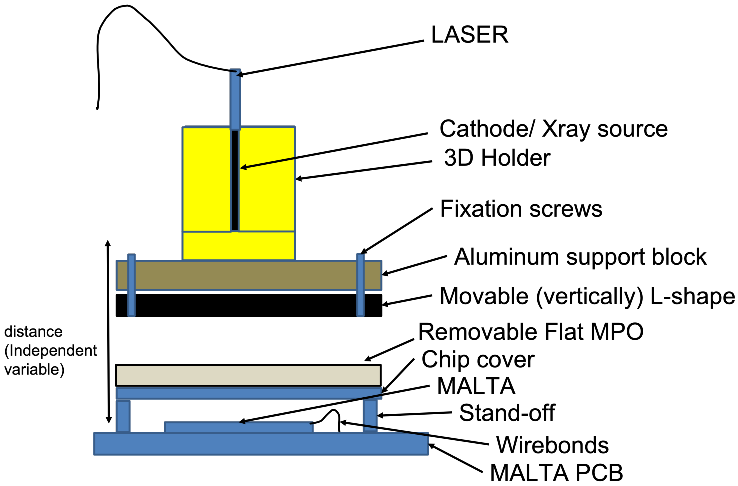

Figure 3: Experimental Set-up

2 Research questions and Methodology

This research tried to provide an answer to the following questions:

1. How do the following variables affect the X-ray detected by MALTA?
   - Source-detector distance
   - MPO-source distance
2. Which set-up would result to the most focused X-ray beam?
   - MPO in 3-D holder
   - MPO in 3-D holder and near MALTA
   - MPO on MALTA

2.1 Set-up

Figure 3 shows the set-up used to investigate and answer the research questions.

Table 1: Run Specifications

Variable	Description	
Vlow	Lowest pulse that the detector was sensitive.	80
Vhigh	Highest pulse that the detector was sensitive.	100
Laser Intensity	Intensity of the pulse emitted by the laser.	1.7
Triggers		50000
Repetitions	Number of iterations	100
Current	Ratings of the voltage source	~8 A
Voltage		~12000 V
IDB	This is the main parameter to change the threshold, a lower value means lower threshold, for too low thresholds the chip goes into oscillation)	100

Table 2: Divergence Angle and Focusing Capability Data

		MPO Holder		MPO Holder and Malta		MPO Malta		No MPO	
Distance of the platform	holder type	Entries	Std deviation (pixels)	Entries	Std deviation (pixels)	Entries	Std deviation (pixels)	Entries	Std deviation (pixels)
5 cm	A (+1.6cm)	64486	99.67	1917	31.22	43398	57.68	na*	na*
	B (+3.2cm)	89528	111.9	1777	34.245	41939	56.3	na*	na*
	C (+4.8cm)	134930	130.45	1593	37.98	40411	55.31	na*	na*
10 cm	A (+1.6cm)	37303	109.92	1716	40.4	37115	59.54	3347751	149.1
	B (+3.2cm)	61595	132.4	1577	41.48	35447	59.27	2843497	148.8
	C (+4.8cm)	75501	143.7	1313	42.79	34311	59.51	2408802	148.6
15 cm	A (+1.6cm)	34898	133.3	1373	46.37	32473	63.15	1619998	148.3
	B (+3.2cm)	39135	140.25	1354	50.05	31344	63.9	1414187	148.2
	C (+4.8cm)	43178	147.4	1196	55.05	30892	65.07	1249360	148.15
20 cm	A (+1.6cm)	22653	140.6	1141	57.38	28835	68.825	866961	147.85
	B (+3.2cm)	24611	146.15	1191	58.19	28238	70.015	770898	147.95
	C (+4.8cm)	24088	148.6	944	58.06	27312	71.195	704459	147.9

na*- saturated detector

The aluminum support block was moved to change the distance between the X-ray source and the MALTA detector. The 3D holder was fabricated to hold the small MPO. There are three 3D holders (Holder A, Holder B, Holder C) used with varying distance between the small MPO and the X-ray source in order to see how the MPO-source is related to the focusing capability. Finally, the flat MPO near MALTA is removable to determine whether it is better to use a single MPO or two MPOs. Table 1 shows the run specifications. The variables in this table are what were set to be constants.

3 Results and Discussion

3.1 Varying Source-detector Distance

Table 2 shows the data of varying the distance between the detector and the source with the four set-ups: MPO in the holder, MPO Holder and MALTA, MPO near MALTA, and no MPO. When the X-ray source is very close to MALTA, there will be no reading because it is being saturated. In figure 4, it can be seen how the entries vary depending on the distance of the source and MALTA.

All set-ups show that the number of entries varies inversely with distance. The entries received by MALTA decreases whenever an MPO is placed between it and the source. The number of entries

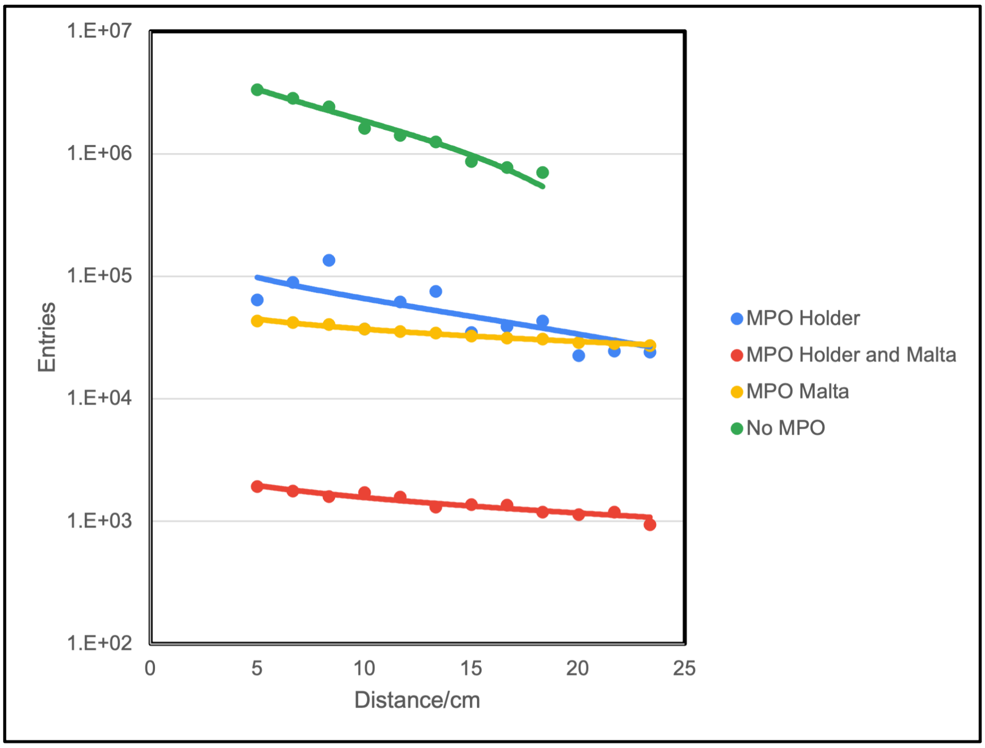

Figure 4: Entries vs. Distance

significantly decreases as you put MPO between the source and the detector. A single MPO has approximately 10 to 100 times more entries than a two-MPO set-up. This suggests that the MPOs manifest reflection or attenuation of X-ray photons.

To look at how clustered the entries are, the standard deviation for each set-up was computed. Figure 5 shows how the standard deviation varies with distance for each set-up. The no MPO set-up almost show a horizontal line for this graph suggesting that the standard deviation does not vary with distance. As it can be seen in Table 2, the standard deviations for no MPO set-up are almost equal to each other. This means that the probability of an X-ray photon hitting a pixel in MALTA is the same for all other pixels. For further visualization, figure 6 shows the 3D histogram for three distances for no-MPO set-up.

The X-ray hits decreased when an MPO is placed at the MPO holder. Also, SD continuously increased when the distance increases. There is also a point where the SD is comparable to when there is no MPO. It can also be seen from Figure 7 how the clustering of the radiation varies with distance in this set-up. In this set-up, X-rays are more focused when the source is placed near MALTA.

The third set-up is when the MPO is placed near MALTA. It garnered a significantly lower SD than when the MPO is placed near the source. Furthermore, the X-rays are more focused when the source is placed near MALTA. The trend also shows that the SD increases when the source gets farther to the detector. Visualization of the radiation detected by MALTA is shown in Figure 8.

Figure 9 shows how the X-rays are characterized by MALTA when two MPOs are placed between the detector and the source. One MPO is placed near the source and the other MPO is placed near MALTA. This set-up garnered the lowest entries but with the most focused X-ray, as it can be seen in figure 4. The first MPO might have focused the X-ray photons and further focused by the MPO near MALTA. Another notable point of analysis are the peaks at the sides of the focus points. This might be attributed to possible intensified scattering.

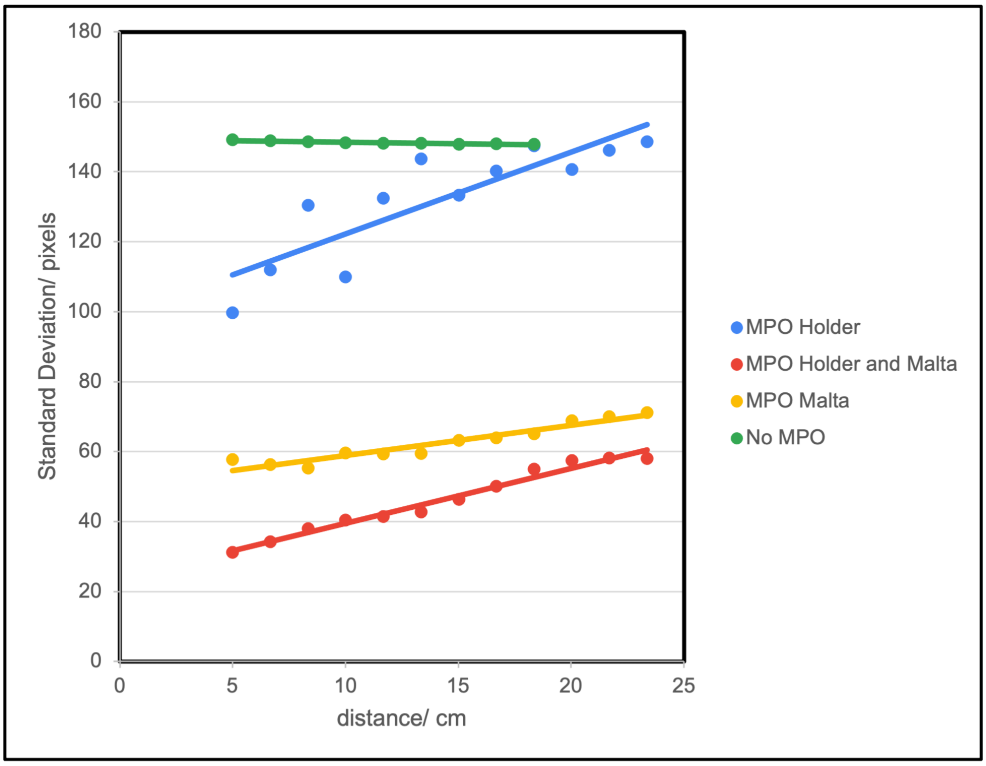

Figure 5: Standard Deviation vs. Distance

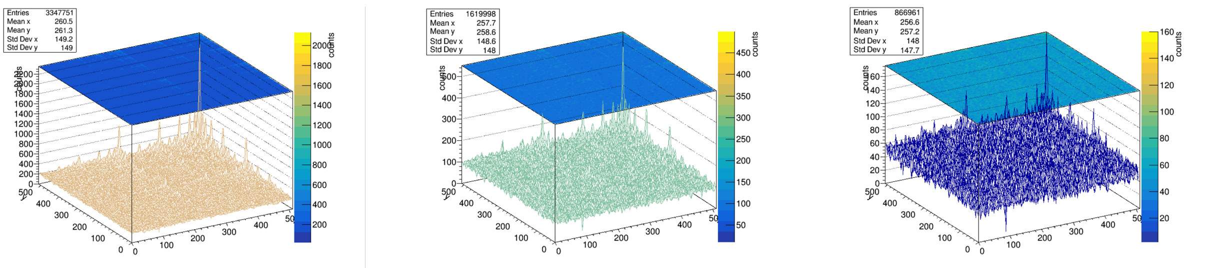

(a) 5cm (b) 10cm (c) 20cm

Figure 6: Histogram for No MPO set-up

3.2 Varying MPO-Source Distance

The effects of the MPO-Source distance were investigated by using three different holders with varying heights, as shown in figure 10. Figure 11 shows how the MALTA detected the X-rays when the MPO is placed near the source. The distances between the source and MALTA are set to be constants. The X-rays are more clustered when using holder A. Figure 12 also shows how the SD varies with source-detector distance for each holder. Holder A has the smallest distance from the source and the MPO and it provided the smallest standard deviation. This suggests that the closer the MPO to the source, the smaller the divergence.

3.3 Divergence Angle and Focusing Capability

Figure 13 defines the divergence angle (theta). This was computed to determine by how much the X-rays diverge from the window of the source. The divergence angles for each set-up was measured using SD

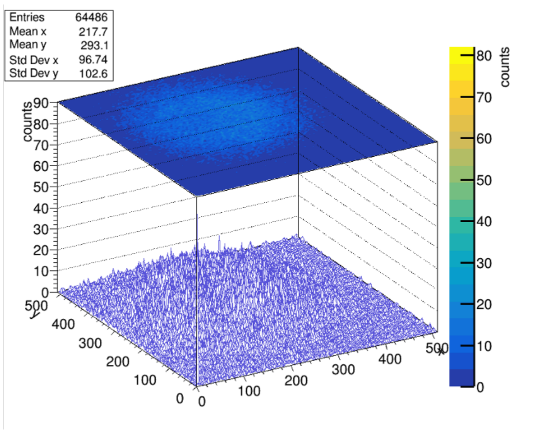

(a) 5cm

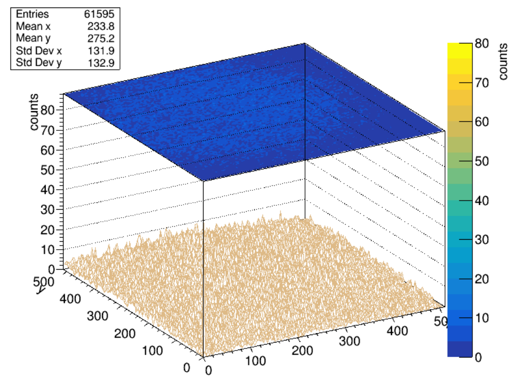

(b) 10cm

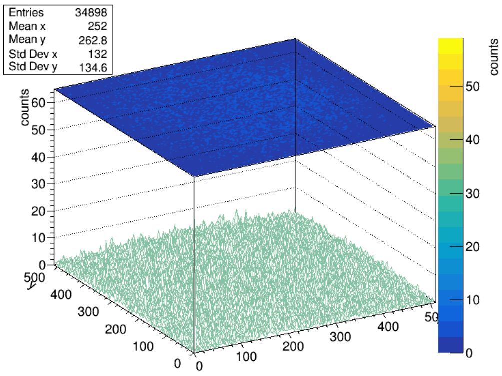

(c) 20cm

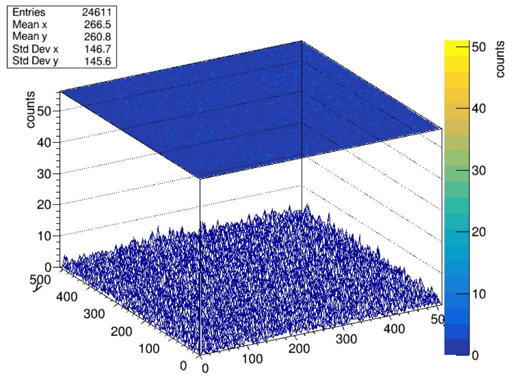

(d) 20cm

Figure 7: Histograms for MPO Holder set-up

Table 3: Divergence Angle and Focusing Capability Data

Distance	MPO holder			MPO holder and malta			MPO malta			no MPO	
	SD (cm)	Divergence (degrees)	Focusing capability (%)	SD (cm)	Divergence (degrees)	Focusing capability (%)	SD (cm)	Divergence (degrees)	Focusing capability (%)	SD (cm)	Divergence (degrees)
10.01	0.66	3.79	26.19	0.24	1.39	72.84	0.36	2.05	59.98	0.90	5.13
11.68	0.80	3.91	10.99	0.25	1.23	72.07	0.36	1.75	60.10	0.90	4.39
13.35	0.87	3.71	3.29	0.26	1.11	71.16	0.36	1.54	59.90	0.90	3.84
15.02	0.80	3.06	10.09	0.28	1.07	68.70	0.38	1.45	57.38	0.89	3.41
16.69	0.85	2.90	5.35	0.30	1.04	66.20	0.39	1.32	56.85	0.89	3.06
18.36	0.89	2.77	0.51	0.33	1.04	62.82	0.39	1.22	56.05	0.89	2.79
20.03	0.85	2.42	4.90	0.35	0.99	61.17	0.42	1.19	53.43	0.89	2.55
21.70	0.88	2.33	1.22	0.35	0.93	60.65	0.42	1.11	52.66	0.89	2.35
23.37	0.90	2.20	-0.47	0.35	0.86	60.73	0.43	1.05	51.84	0.89	2.19
AVERAGE FOCUSING CAPABILITY			**6.90**			**66.26**			**56.46**		

of the entries. The divergence angles are compared to the divergence angle of the non-MPO set-ups. The distances where the detector was saturated where not used in this analysis. The focusing capability (FC), in percent, is defined as the ability of the set-up to focus the X-ray as compared to the a non-MPO set-up. It is solved using the equation

$$FC = 100 - (\theta_{set-up} - \theta_{non-MPO}) \tag{2}$$

.

Table 3 shows the divergence angle and FC for each set-up. Since the SD for the no-MPO set up

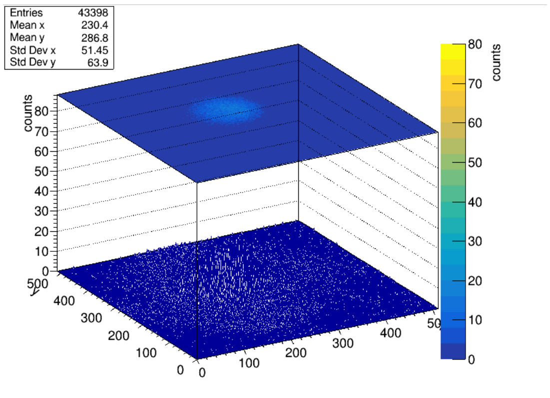

(a) 5cm

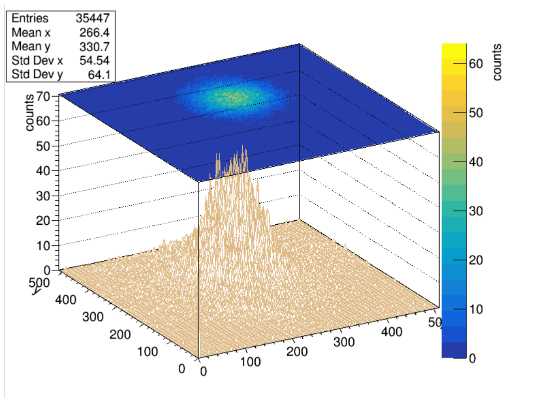

(b) 10cm

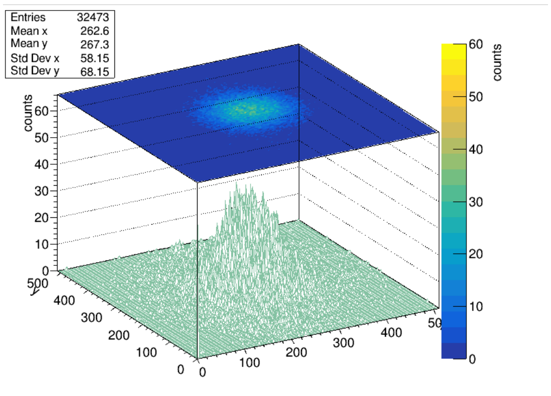

(c) 20cm

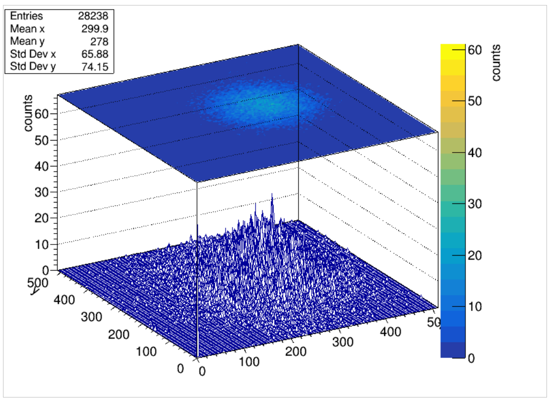

(d) 20cm

Figure 8: Histograms for MPO on MALTA set-up

is almost equal for each distance, it can be expected that the divergence angle decreases as the distance between the source and the detector increases. The set-up that got the highest focusing capability is the two-MPO set-up. When two MPOs are used- one near the source and one near MALTA, the X-ray will be 66% more than when there is no MPO used.

Using a single MPO had slower focusing capability. The MPO placed near the source set-up was not very effective in focusing X-rays. When the source and the detector are far from each other, this set-up behaves like a no-MPO set-up. It is also noticeable in table 3 that it had a negative FC because it is worse than a no MPO set-up in that specific distance. On the other hand, for a single MPO placed near MALTA, the FC is 56%. This is a more significant FC than the previous set-up.

As coherent in table 3, figure 14 shows that, given the distances, using two MPOs yielded 10% more focusing capability than when using just MPO near MALTA and 50% more when using MPO in the holder. For a single-MPO set-up, it is better if the MPO is placed near the detector. It is noticeable that the MPO-holder setup yielded a low focusing capability compared to when the MPO is placed near the MALTA. When the MPO is placed very far from the detector, the X-rays tend to diverge comparable to a non-MPO set-up. This is being manifested by the negative value of the focusing capability of the MPO-holder set-up.

4 Conclusions

Varying the source-detector distance and MPO-source distance affected both the amount of hits and the X-ray deviation detected by MALTA. As the source- detector increases, the number of hits decreases.

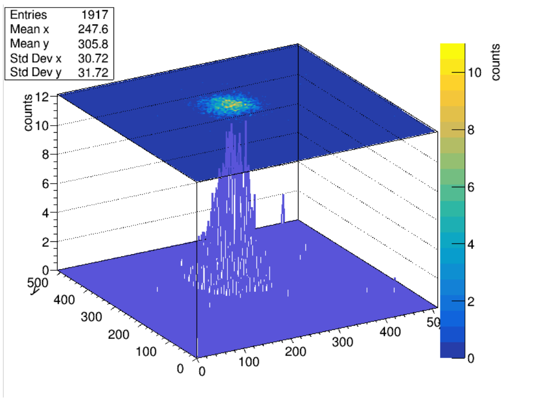

(a) 5cm

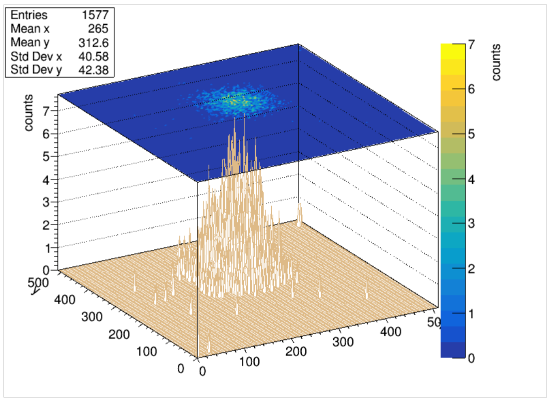

(b) 10cm

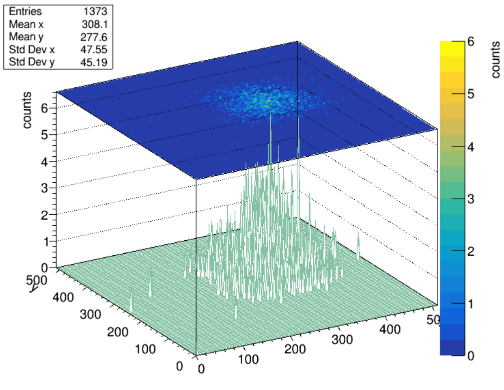

(c) 20cm

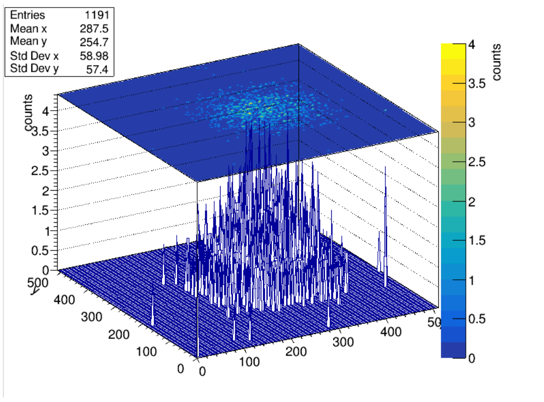

(d) 20cm

Figure 9: Histograms for MPO in Holder and on MALTA set-up

Figure 10: (left) Holder A, (middle) Holder B, (right) Holder C

Source-detector distance (cm)	Holder A	Holder B	Holder C
5	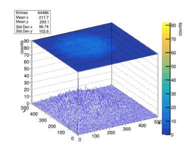	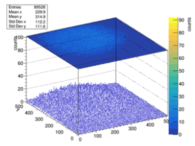	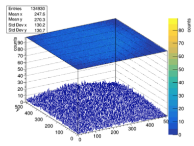
10	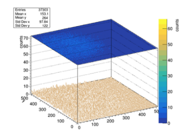	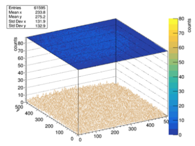	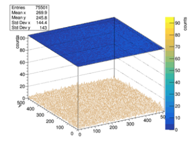
15	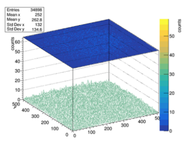	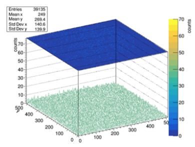	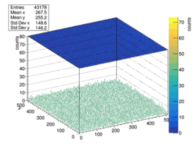
20	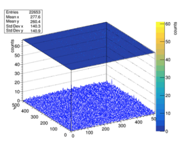	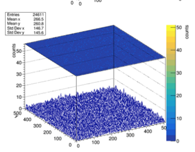	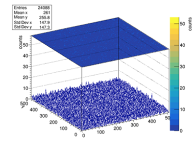

Figure 11: Histogram for each MPO holder

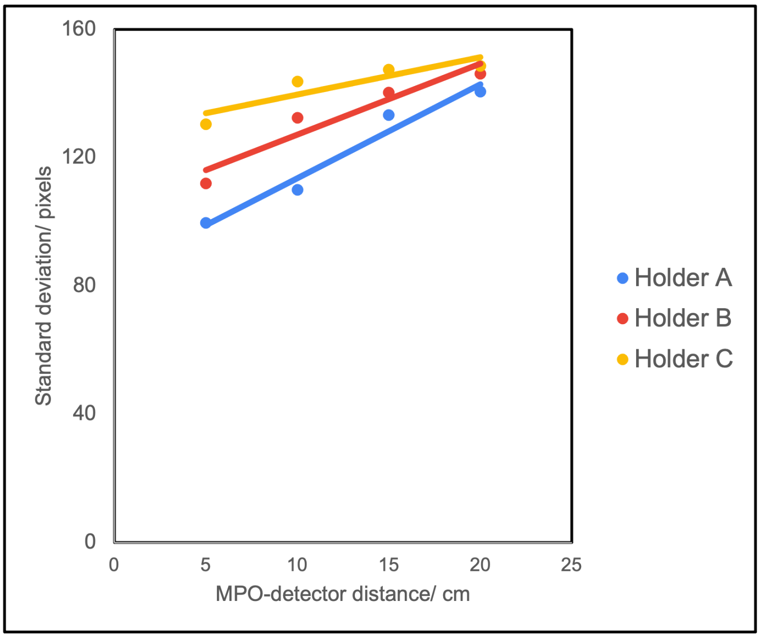

Figure 12: Effect of MPO-source Distance to Standard Deviation

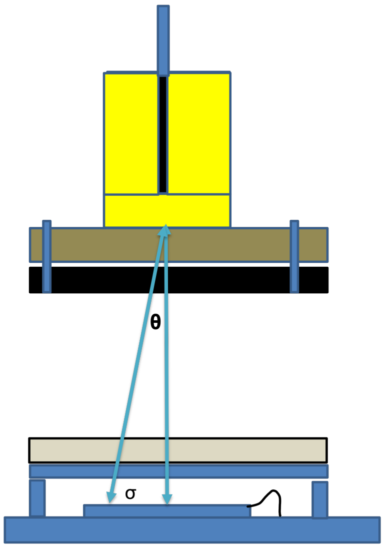

Figure 13: Divergence Angle Definition

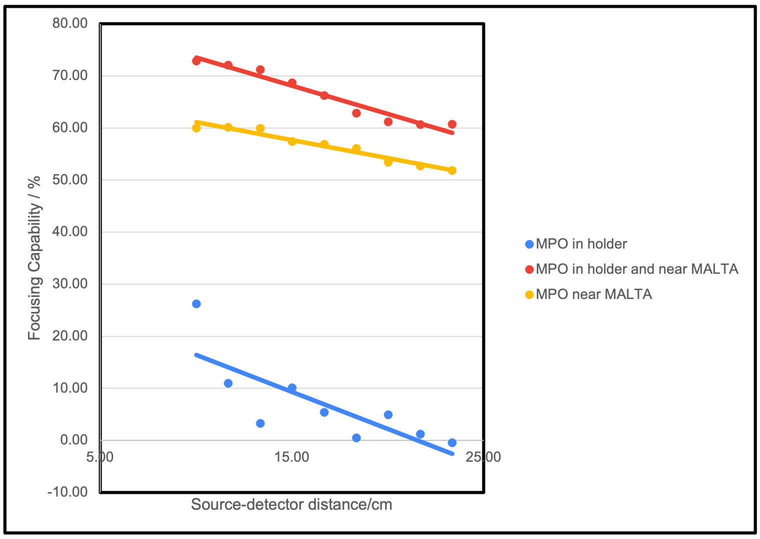

Figure 14: Focusing Capability Trend

This can be attributed to divergence of the X-ray photons. When an MPO is inserted near the source, the number of hits decreases by a factor of 10^1.The number of hits further decreased by the same factor when another MPO is placed near MALTA. The MPO-source distance affected the deviation of the X-ray photons. X-rays are more focused when the MPO is placed very near the source. However, among the set-ups used in this research, placing the MPO near the source yielded the least focusing capability of just 6%. The best way of focusing the X-rays is by placing two MPOs, one near the source and one near the detector. This set-up yielded an average focusing capability of 66%. Placing an MPO near MALTA garnered an average focusing capability of 56%.

Bibliography

[1] H. Li *et al.*, “Micro-computed tomography for small animal imaging: Technological details,” *Progress in Natural Science*, vol. 18, no. 5, pp. 513–521, 2008.

[2] H. Pernegger *et al.*, "Radiation hard monolithic CMOS sensors with small electrodes for High Luminosity LHC," *Nucl. Instrum. Methods. Phys. Res. A*, vol. 986, p. 164381, 2021.

[3] K. Wallace *et al.*, "Development of micro-pore optics for x-ray applications," in *Optics for EUV, X-Ray, and Gamma-Ray Astronomy II* (O. Citterio and S. L. O'Dell, eds.), vol. 5900, pp. 309 – 318, International Society for Optics and Photonics, SPIE, 2005.